ChemComm

COMMUNICATION

View Article Online
View Journal | View Issue

Cite this: *Chem. Commun.*, 2015, **51**, 12470

Received 16th June 2015,
Accepted 29th June 2015

DOI: 10.1039/c5cc04982b

www.rsc.org/chemcomm

Supramolecular chirality in self-assembled peptide amphiphile nanostructures†

Ruslan Garifullin and Mustafa O. Guler*

Induced supramolecular chirality was investigated in the self-assembled peptide amphiphile (PA) nanosystems. Having shown that peptide chirality can be transferred to the covalently-attached achiral pyrene moiety upon PA self-assembly, the chiral information is transferred to molecular pyrene *via* weak noncovalent interactions. In the first design of a supramolecular chiral system, the chromophore was covalently attached to a peptide sequence (VVAGH) *via* an ε-aminohexanoic acid spacer. Covalent attachment yielded a PA molecule self-assembling into nanofibers. In the second design, the chromophore was encapsulated within the hydrophobic core of self-assembled nanofibers of another PA consisting of the same peptide sequence attached to lauric acid. We observed that supramolecular chirality was induced in the chromophore by PA assembly into chiral nanostructures, whether it was covalently attached, or noncovalently bound.

The induced chirality phenomenon is exploited for monitoring DNA hybridization in real time,[1] determination of absolute configuration of molecules by zinc phthalocyanine tweezers,[2] and synthesis of chiral plasmonic nanostructures.[3] Chiral centers in macromolecules can induce chiral order in supramolecular ensembles of the same molecules. Even a single chiral center can impact a final supramolecular chirality. Several studies by Meijer[4–7] and Stupp[8] groups have shown that a chiral center in an alkyl group of a molecule can affect the overall helicity of a supramolecular polymer. It was also observed that chiral molecules could induce chiral organization of achiral molecules by strong noncovalent interactions, such as electrostatic and coordination interactions; thus representing an interesting tool for control of materials' properties.[9–11]

Chiral molecules such as peptides are interesting model structures for studying induced chirality. All of the natural amino acids, except glycine, used in mRNA translation are chiral; therefore polypeptides are intrinsically chiral. Molecular chirality of peptides can be used to induce supramolecular chirality upon assembly of individual molecules into one-dimensional nanostructures.[12–14] Effective assembly of this type can be achieved when a certain peptide sequence is attached to a hydrophobic fatty acid. Aliphatic peptide amphiphiles (PAs) possess this type of design and exhibit self-assembly properties. Aliphatic PAs comprise an oligopeptide sequence and a covalently attached aliphatic tail, which is typically 12–16 carbon atoms long.[15] PAs can self-assemble into various nanostructures such as nanoribbons, nanofibers and micelles[16] depending on their amino acid sequence and aliphatic tail.

Here we exploited nanofiber forming PAs, because nanofiber formation leads to helical arrangement of individual PA molecules along the nanofiber axis.[17] Helical arrangement stems from the twisted geometry of β-sheets forming the PA nanofibers; nevertheless, helicity is not translated into fiber morphology and lateral stacking of β-sheets interdigitated along hydrophobic tails leads to almost flat nanofibers with helical interior. Nanofibers formed from all-L and all-D peptide isomers are expected to possess left- and right-handed interior, respectively. However, there are some reports on handedness inversion in peptide and protein based nanofibers.[18,19] As shown here, this type of arrangement forces covalently attached or noncovalently encapsulated chromophore molecules to exhibit induced chirality. The letter case represented by encapsulated chromophore is of great importance, because it arises solely based on weak noncovalent interactions such as solvophobic effect and van der Waals forces. By manipulating amino acid sequence from all-L to all-D, it is possible to control chiroptical properties of a chromophore. It is achievable to choose whether left or right circularly polarized light will be absorbed. This choice manifests itself in a switch of the sign of induced peaks in circular dichroism (CD) spectra.

In this study, we developed two strategies, which allowed inducing supramolecular chirality with an achiral pyrene chromophore. The first strategy included the covalent attachment of the chromophore to all-L and all-D variants of the same peptide sequence (VVAGH) and formation of self-assembled nanofibers of **1** and **1′** (Fig. 1). For this purpose, pyrenebutyric acid was covalently attached to the peptide sequence *via* an ε-aminohexanoic acid spacer. The second strategy

Institute of Materials Science and Nanotechnology, National Nanotechnology Research Center (UNAM), Bilkent University, Ankara 06800, Turkey.
E-mail: moguler@unam.bilkent.edu.tr

† Electronic supplementary information (ESI) available: Details of experimental information. See DOI: 10.1039/c5cc04982b

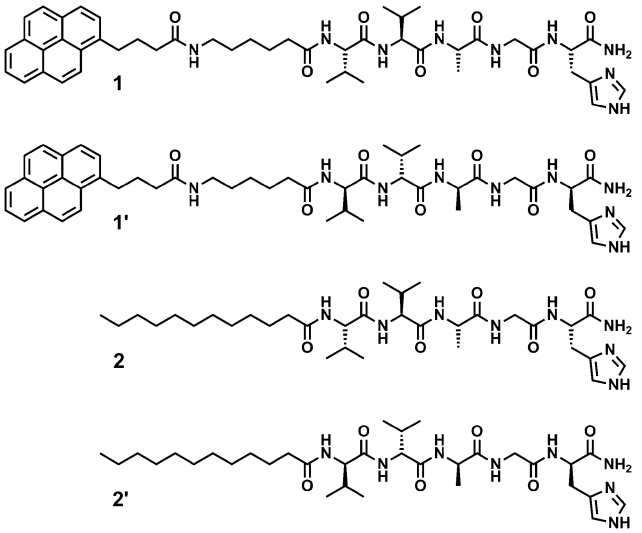

Fig. 1 Structural formula of pyrenebutyryl-ε-Ahx-VVAGH-Am (**1**), pyrenebutyryl-ε-Ahx-VVAGH-Am (**1′**), lauryl-VVAGH-Am (**2**), and lauryl-VVAGH-Am (**2′**).

included noncovalent encapsulation of the chromophore in self-assembled nanofibers of **2** and **2′**, which are all-L and all-D variants of the VVAGH peptide sequence next to lauric acid (Fig. 1).

The peptides were synthesized by the Fmoc solid phase peptide synthesis method.[20] The molecules were obtained with high purities and purities were identified by liquid chromatography – mass spectroscopy analysis (Fig. S1–S8, ESI†). During liquid chromatography, all of the peptides were traced at 220 nm, and peptides **1** and **1′** were additionally traced at 335 nm (pyrene moiety absorption region). Peaks observed in chromatograms matched exact mass peaks in mass spectra. Synthesized peptides were designed to self-assemble into one-dimensional nanostructures.[21] Three-domain amphiphile design was utilized to achieve the self-assembly process. The first segment is a hydrophilic head consisting of histidine residue (H), the second one is a hydrophobic β-sheet promoting peptide sequence (VVAG), and the last one is a hydrophobic tail. This self-assembly property was used to chirally organize a structurally achiral chromophore.

In both of the chiral order induction strategies, nanofiber formation was driven by the solvophobic effect.[21,22] Solvophobic collapse of PAs is enhanced by effective H-bonding between β-sheet forming peptide segments (VVAG). The hydrophilic histidine residue leads to solubilization of the self-assembled nanofibers in water. Spatial organization of the PA molecules in the nanofibrous structures (**1**–**2′**) determines the chiroptical features of the chromophore. Structurally achiral chromophore starts to behave as if it was chiral, it can be proposed that chromophore is forced to arrange in a chiral manner.

Covalent attachment of the chromophore was used to observe induced supramolecular chirality of **1** and **1′** nanofibers. TEM images revelaed assembly of **1** and **1′** into nanofibers (Fig. 2a and b); spatial organization of PA molecules throughout the nanofiber dictates helical organization of chromophores within hydrophobic core. In order to verify the presence of chiral order, emission and circular dichroism spectra were recorded for covalently attached

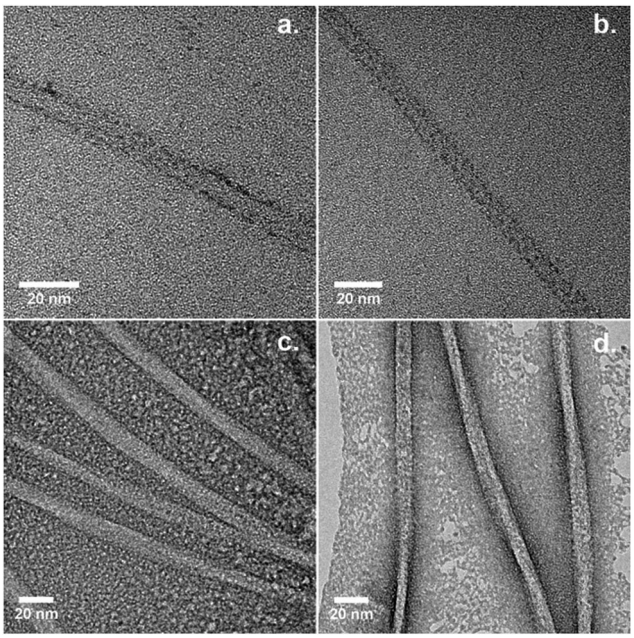

Fig. 2 TEM images of self-assembled nanofibers of (a) **1** and (b) **1′**, (c) **2** and (d) **2′**.

pyrene samples (**1** and **1′**). First, emission spectra revealed that chromophores are organized in the hydrophobic core of PAs as ratio of the vibronic peaks (I_3/I_1) in the spectra of pyrene moiety is greater than unity (Fig. 3a and b).[23] The ratio of vibronic peaks in the spectra of strongly hydrophobic pyrene is frequently used to probe its environment; the value of I_3/I_1 ratio is generally greater than unity for hydrophobic environments, and less than unity for hydrophilic ones. Second, π–π stacking of the chromophores is evident from excimer formation at 460 nm in emission spectra of pyrene (Fig. 3a and b).[24] Induced peaks (230–400 nm) in the CD spectra also point toward spatially chiral organization of the chromophores (Fig. 4a); bisignate signals (Cotton effect) between 195–230 nm in the same spectra are indication of PA assembly with twisted β-sheet motif.[25,26] Furthermore, pyrene conjugated peptides were directly dissolved in trifluoroethanol (TFE) and emission spectra were recorded (Fig. 3a and b). We observed that the ratio of vibronic peaks (I_3/I_1) in pyrene emission spectra is smaller than unity, which means that pyrene moiety is in hydrophilic medium and completely solvated in TFE. Absence of excimer peaks also points toward solvated peptides. CD spectra (Fig. S9a, ESI†) of the same samples also suggest that peptide

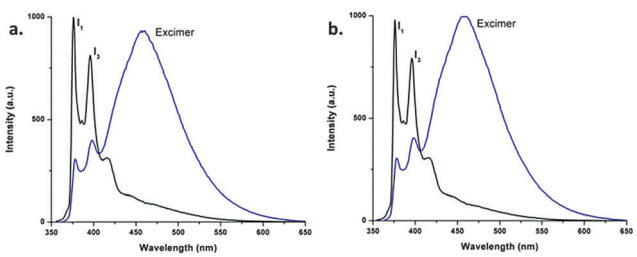

Fig. 3 Emission spectra of (a) **1** and (b) **1′** in H_2O (blue) and trifluoroethanol (black).

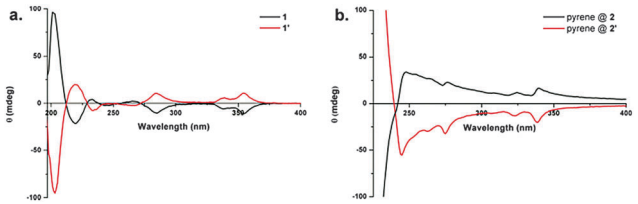

Fig. 4 CD spectra of self-assembled PA nanofibers of (a) **1** and **1′**, (b) **2** and **2′** with encapsulated pyrene in H_2O (0.333 mM pyrene).

molecules are not assembled, because there are no induced CD peaks in pyrene absorption region (230–400 nm). The only peak present is a broad peak around 220 nm, which shows that β-sheet formation is disrupted and disordered interactions are dominant. Similarly, when the aqueous solutions (3.33 mM) containing self-assembled nanofibers of **1** and **1′** were diluted 10 times with trifluorethanol (TFE), induced CD signals in pyrene absorption region disappeared (Fig. S9b, ESI†). Moreover, the peak centered at *ca.* 220 nm appeared, thus representing shift of the system from β-sheet dominant state to random state. Another intriguing observation was that a bathochromic shift with a value of greater than 10 nm was observed when absorption spectra of **1** and **1′** in TFE were compared to the spectra of the same in H_2O (Fig. S10 and S11, ESI†). This shift is indicative of J-aggregate formation.[27] Bulky amino acid sequence seems to interfere with π–π stacking process and result in slipped stacks.

The second strategy used to induce supramolecular chirality involves encapsulation of pyrene molecules by **2** and **2′**. Previously, we observed that lauryl-VVAGH-Am (**2**) effectively encapsulates a zinc phthalocyanine derivative by forming nanofibers.[28] In the same manner, ensapsulation of pyrene by PA molecules **2** and **2′** is expected to result in nanofiber formation and in induction of supramolecular chirality. Indeed, TEM images showed the formation of tapered nanofibers (Fig. 2c and d), whose helical interior should direct organization of encapsulated chromophore molecules. Induced CD peaks with opposite signs were observed for pyrene encapsulated in nanofibers of **2** and **2′** (Fig. 4b). The β-sheet signals originating from peptide interactions were also observed (Fig. S12, ESI†). CD spectrum of pyrene dissolved in tetrahydrofuran (THF) did not exhibit any induced chiral peaks (Fig. S13, ESI†). Moreover, emission spectra (Fig. S14, ESI†) of encapsulated pyrene systems show similar results to pyrene conjugated PAs. In other words, the ratio of vibronic peaks (I_3/I_1) is greater than unity and the excimer peak due to π–π stacking is present at 460 nm. On the other hand, pyrene dissolved in THF did not exhibit excimer emission (Fig. S15, ESI†). Peptides **2** and **2′** do not fluoresce on their own, emission was not detected neither in assembled form in H_2O nor in dissolved form in TFE (Fig. S16a and b, ESI†). In addition, absorption spectra of encapsulated pyrene exhibits a slight bathochromic shift (Fig. S17, ESI†), which is indicative of weaker J-aggregate formation. Based on these observations it can be inferred that the encapsulated chromophore is forced to acquire chiral three-dimensional arrangement along the PA nanofiber. Induced helical organization of the system, left- or right-handed, is arguably the best three-dimensional arrangement that accounts for observed induced peaks in CD spectra. It should be noted that PAs **2** and **2′** when assembled in aqueous medium on their own (without pyrene) form twisted nanoribbons (Fig. S18, ESI†) rather than nanofibers. A few nanoribbons were observed in samples with encapsulated pyrene (Fig. S19, ESI†). It can be speculated that simultaneous assembly of pyrene and PA molecules affects final morphology of nanostructures. Solvophobic collapse of the PAs creates highly hydrophobic regions in emerging nanostructures. These regions tend to accommodate hydrophobic pyrene molecules, which in their turn facilitate further nanostructure growth. In this way, supramolecular systems where pyrene molecules are surrounded by PA molecules converge to supramolecular nanosystems where pyrene is directly attached to chiral peptide sequence.

In conclusion, we have seen that supramolecular chirality is induced in the chromophores by chiral PA assembly, whether they are covalently attached, or noncovalently bound. Both of the strategies led to induction of chiral signals in CD spectra. CD spectra along with emission spectra suggest that chromophores are organized in a helical manner in the core of nanofibers. Chiral signals in the pyrene moiety/molecule absorption region unveiled the chiral organization of the chromophores. Excimer peaks in the emission spectra of the nanosystems suggested chromophore stacking; moreover, the ratio of vibronic peaks in the spectra suggested that the chromophores are situated in a hydrophobic environment, presumably the hydrophobic core of the peptide nanofibers. In addition, bathochromic shifts in absorption spectra point toward slipped stacks of the pyrene moieties or pyrene molecules. Based on these observations, mutual orientation of the chromophores in a helical manner is arguably the best explanation for chirally stacked chromophores throughout the nanofiber core. Interestingly, induced chiral peaks in CD spectra can be controlled by changing the peptide sequence from all-L to all-D design, thus establishing control over chiroptical properties of the chromophore. Importantly, the nanosystems with noncovalently bound pyrene represent an approach, which exploits weak noncovalent interactions. Individual weak interactions such as hydrophobic and van der Waals interactions are amplified *via* self-assembly into nanostructures, thus realizing chirality transfer from chiral PA molecules to the achiral chromophore.

We acknowledge TÜBİTAK-BİDEB for PhD fellowship (2215) granted to R.G. This work was supported by TÜBİTAK 114Z728.

Notes and references

1 Y. Tang, K. E. Achyuthan and D. G. Whitten, *Langmuir*, 2009, **26**, 6832–6837.
2 X. Huang, B. H. Rickman, B. Borhan, N. Berova and K. Nakanishi, *J. Am. Chem. Soc.*, 1998, **120**, 6185–6186.
3 A. Kuzyk, R. Schreiber, Z. Fan, G. Pardatscher, E.-M. Roller, A. Hogele, F. C. Simmel, A. O. Govorov and T. Liedl, *Nature*, 2012, **483**, 311–314.
4 J. van Gestel, A. R. A. Palmans, B. Titulaer, J. A. J. M. Vekemans and E. W. Meijer, *J. Am. Chem. Soc.*, 2005, **127**, 5490–5494.
5 M. M. J. Smulders, P. J. M. Stals, T. Mes, T. F. E. Paffen, A. P. H. J. Schenning, A. R. A. Palmans and E. W. Meijer, *J. Am. Chem. Soc.*, 2010, **132**, 620–626.
6 A. J. Markvoort, H. M. M. ten Eikelder, P. A. J. Hilbers, T. F. A. de Greef and E. W. Meijer, *Nat. Commun.*, 2011, **2**, 509.
7 F. Wang, M. A. J. Gillissen, P. J. M. Stals, A. R. A. Palmans and E. W. Meijer, *Chem. – Eur. J.*, 2012, **18**, 11761–11770.

8 B. W. Messmore, P. A. Sukerkar and S. I. Stupp, *J. Am. Chem. Soc.*, 2005, **127**, 7992–7993.
9 E. Bellacchio, R. Lauceri, S. Gurrieri, L. M. Scolaro, A. Romeo and R. Purrello, *J. Am. Chem. Soc.*, 1998, **120**, 12353–12354.
10 R. Oda, I. Huc, M. Schmutz, S. J. Candau and F. C. MacKintosh, *Nature*, 1999, **399**, 566–569.
11 M. Fujiki, *Symmetry*, 2014, **6**, 677–703.
12 Y. Kamikawa and T. Kato, *Org. Lett.*, 2006, **8**, 2463–2466.
13 B. M. Rosen, M. Peterca, K. Morimitsu, A. E. Dulcey, P. Leowanawat, A.-M. Resmerita, M. R. Imam and V. Percec, *J. Am. Chem. Soc.*, 2011, **133**, 5135–5151.
14 U. Lewandowska, W. Zajaczkowski, L. Chen, F. Bouillière, D. Wang, K. Koynov, W. Pisula, K. Müllen and H. Wennemers, *Angew. Chem., Int. Ed.*, 2014, **53**, 12537–12541.
15 J. Castillo, L. Sasso and W. E. Svendsen, *Self-Assembled Peptide Nanostructures: Advances and Applications in Nanobiotechnology*, Pan Stanford, 2012.
16 M. O. Guler, R. C. Claussen and S. I. Stupp, *J. Mater. Chem.*, 2005, **15**, 4507–4512.
17 E. T. Pashuck, H. Cui and S. I. Stupp, *J. Am. Chem. Soc.*, 2010, **132**, 6041–6046.
18 I. Usov, J. Adamcik and R. Mezzenga, *ACS Nano*, 2013, **7**, 10465–10474.
19 C. Lara, N. P. Reynolds, J. T. Berryman, A. Xu, A. Zhang and R. Mezzenga, *J. Am. Chem. Soc.*, 2014, **136**, 4732–4739.
20 W. Chan and P. White, *Fmoc Solid Phase Peptide Synthesis: A Practical Approach*, OUP Oxford, 2000.
21 L. C. Palmer, Y. S. Velichko, M. Olvera de la Cruz and S. I. Stupp, *Philos. Trans. R. Soc., A*, 2007, **365**, 1417–1433.
22 I. W. Fu, C. B. Markegard, B. K. Chu and H. D. Nguyen, *Langmuir*, 2014, **30**, 7745–7754.
23 K. Kalyanasundaram and J. K. Thomas, *J. Am. Chem. Soc.*, 1977, **99**, 2039–2044.
24 T. Förster, *Angew. Chem., Int. Ed. Engl.*, 1969, **8**, 333–343.
25 M. C. Manning, M. Illangasekare and R. W. Woody, *Biophys. Chem.*, 1988, **31**, 77–86.
26 D. W. Weatherford and F. R. Salemme, *Proc. Natl. Acad. Sci. U. S. A.*, 1979, **76**, 19–23.
27 M. Kasha, H. R. Rawls and A. El-Bayoumi, *Pure Appl. Chem.*, 1965, **11**, 371–392.
28 R. Garifullin, T. S. Erkal, S. Tekin, B. Ortac, A. G. Gurek, V. Ahsen, H. G. Yaglioglu, A. Elmali and M. O. Guler, *J. Mater. Chem.*, 2012, **22**, 2553–2559.